Ultrahigh Resolution Multicolor Colocalization of Single Fluorescent Nanocrystals.

Xavier Michalet[a], Thilo D. Lacoste[a], Fabien Pinaud[a], Daniel S. Chemla[a,b], A. Paul Alivisatos[a,c], Shimon Weiss[a,b]

[a]Material Sciences Division and [b]Physical Biosciences Division, Lawrence Berkeley National Laboratory, 1 Cyclotron Road, Berkeley, CA 94720; [c]Department of Chemistry, University of California Berkeley, Berkeley, CA 94720

ABSTRACT

A new method for *in vitro* and possibly *in vivo* ultrahigh-resolution colocalization and distance measurement between biomolecules is described, based on semiconductor nanocrystal probes. This ruler bridges the gap between FRET and far-field (or near-field scanning optical microscope) imaging and has a dynamic range from few nanometers to tens of micrometers. The ruler is based on a stage–scanning confocal microscope that allows the simultaneous excitation and localization of the excitation point-spread-function (PSF) of various colors nanocrystals while maintaining perfect registry between the channels. Fit of the observed diffraction and photophysics-limited images of the PSFs with a two-dimensional Gaussian allows one to determine their position with nanometer accuracy. This new high-resolution tool opens new windows in various molecular, cell biology and biotechnology applications.

Keywords: Superresolution, diffraction limit, fluorescence, microscopy, confocal, single molecule, semiconductor nanocrystal, quantum dot.

1. INTRODUCTION

Fluorescence microscopy has become an indispensable tool for biologists, who can now label multiple molecular targets or subcellular compartments specifically using various methods (DNA specific intercalation, antibody recognition, *in vivo* expression of GFP-tagged proteins, etc). The variety of spectrally separated available fluorescent probes is indeed increasing at a constant pace, and the prospect of being able to observe the detailed functions of internal cellular machinery *in vivo* is looking closer. In addition, tremendous progresses have been performed in microscopy instrumentation and data analysis. For instance, laser, optical filter and detector developments have improved the quality and affordability of confocal microscopy, whereas 3D deconvolution techniques have reached a commercial stage and compete with confocal microscopy in terms of resolution, sensitivity and speed [1].

On the other hand, new challenges have to be faced if we are to study the actual spatial and temporal evolution of molecular species during signal transduction, gene expression or other aspects of metabolism at the proper nanometer scale. These goals indeed call for tools allowing the nanometer resolution localization of multicolor, individual fluorescent probes on a time scale compatible with biological phenomena.

Techniques to reach nanometer resolution imaging are still to be developed, but progress toward this goal is steadily made [2-6]. The main obstacle is namely the diffraction limitation of far-field microscopy, which results in a spot-like image (or point-spread-function, PSF) for a point source, the diameter of the spot being typically of the order of the excitation or emission wavelength. However, localization of sufficiently separated point-like sources can be determined with nanometer accuracy, as is well known in the literature [7, 8]. Normally, some care has to be taken of diverse aberrations coming from far-field optics (filters, dichroic mirrors, lenses, etc) and the inhomogeneity of the sample's index of refraction. We have recently demonstrated a method limiting the effect of these aberrations (called ultrahigh-resolution colocalization, UHRC) to a point where they can effectively be neglected.

A second critical aspect to obtain nanometer resolution localization of single fluorescent probes is the photophysics of probes. If observation of individual interacting molecules or organelles is to be achieved,

Nanoparticles and Nanostructured Surfaces: Novel Reporters with Biological Applications, Catherine J. Murphy, Editor, Proceedings of SPIE Vol. 4258 (2001)

the fluorescent probes used to tag them have to be as small and non-perturbative as possible. Single molecule fluorescence (*in vivo* or not) is now a well established field, but nevertheless, one which is limited to very brief observations (at most a few seconds), due to photobleaching of the dyes used. In addition, the need for spectrally separated probes to detect different targets, requires the use of different laser excitation lines, or two-photon excitation, and usually suffers from broad emission spectra of organic dyes.
Semiconductor nanocrystals (NC) are very promising fluorescent probes in this respect [9-11]. They are small (a few nanometers in diameter, and thus comparable in size to an antibody), can be excited with a common wavelength and have narrow emission spectra (30 nm full width at half maximum, FWHM). Several groups including ours are working on NC functionalization in order to make them useful biological fluorescent probes. Here we show that in combination with our ultrahigh-resolution colocalization approach, they potentially could become the ideal probe for the goals set previously.

2. PRINCIPLE OF ULTRAHIGH-RESOLUTION MULTICOLOR COLOCALIZATION

The principle of ultrahigh-resolution colocalization we have recently presented [12] relies on using a closed-loop piezo-stage scanning confocal microscope, a single excitation wavelength and spectrally separable fluorescent probes, as illustrated on Figure 1.

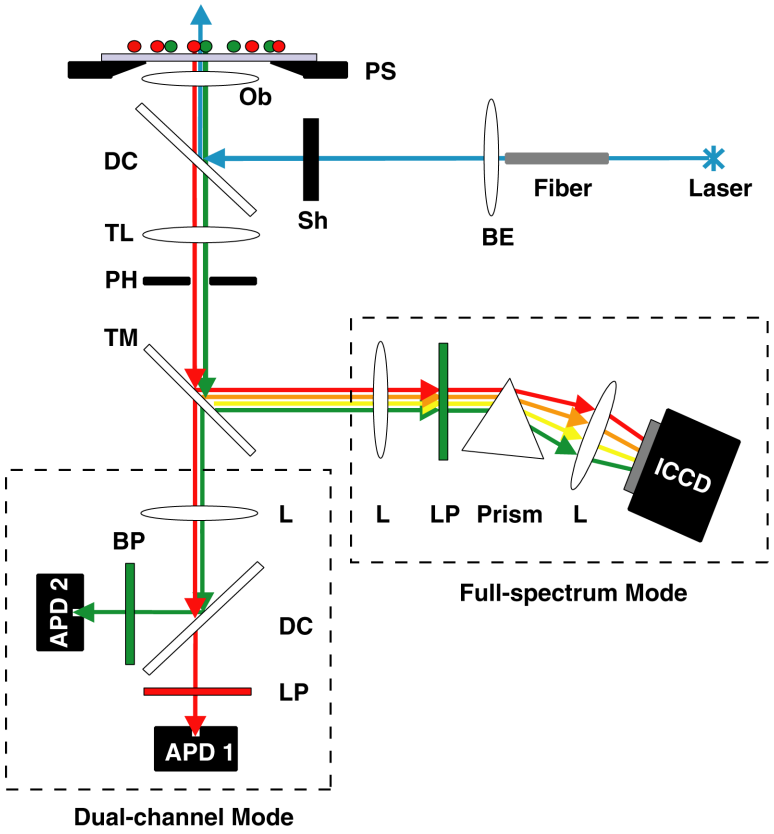

Figure 1: Setup used for ultrahigh-resolution colocalization of multicolor fluorescent probes. The microscope is a homemade stage-scanning confocal microscope using a nanometer-resolution closed-loop piezo-stage scanner (PS). A single laser line is brought via a fiber and a beam expander (BE) to the back focal plane of the objective (Ob) after reflection on a dichroic mirror (DC). Emission of the fluorescent probes is collected by the same objective, and either sent to a dual-channel recording arm using avalanche photodiodes (APD), or to a full-spectrum recording arm using a prism and an intensidifed CCD camera (ICCD). Sh: Shutter, TL: Tube lens, PH: Pinhole, TM: Tiltable Mirror, L: lens, LP: Longpass Filter, BP: Bandpass Filter.

Briefly, moving the sample with nanometer-resolution steps through the fixed on-axis excitation point-spread-function of the microscope objective, the emitted fluorescence is simultaneously recorded at different wavelengths, using either dichroic mirrors, emission filters and avalanche photodiodes (dual-channel mode) or a dispersive prism allowing the emitted spectrum to be focused and imaged onto the chip of an intensified CCD camera (ICCD). Since the excitation PSF is fixed on the optical axis, there is no contribution of off-axis aberrations encountered in beam-scanning confocal microscopy. Moreover, the recorded intensity for each channel is directly proportional to the excitation PSF, the effect of the imaging arm being constant for each emission wavelength, since this emission takes place on-axis.

In the dual-channel acquisition mode (lower part of Fig. 1), two-color APD images were constructed by overlaying the two independent, false-colored channel images. In the full-spectrum mode (lower right part of Fig. 1), the 3-dimensional data set (1 spectral + 2 spatial dimensions) had to be reduced in individual channel images for easier manipulation. A simple approach was used to detect individual spectra of many single NCs. For this, we scanned the spatial recording and summed the 10 nm-binned spectra of each block of n x n pixels, where n is chosen in such a way that the block covers an area corresponding to the PSF extension. We summed these histograms and used the spectral peaks observed in the resulting histogram as central wavelengths for the filtering step.
In the next step, spectral bands (typically 25 nm width) centered on the previously extracted peaks were used to generate images from the original data set. From these images, the binned spectra of detected NCs were determined as explained previously, with the block of pixels centered on the approximate position of the observed NCs.
In the third step, narrower spectral bands (5-20 nm) were chosen to define new color channels with reduced spectral overlaps (i.e. as 'orthogonal' as possible). In the fourth step, the above images were combined into a composite false-color image with perfect registry between each color plane. These composite images are the multicolor equivalent of the dual-color images obtained on the dual-channel APD detection mode.

The final steps of the UHRC analysis consist in determining the position of each PSF's center. This is done using a now classical 2D Gaussian fitting approach [8, 13-16]. Numerical simulations as well as theoretical arguments show that nanometer resolution can be achieved for sufficiently large signal-to-noise ratio (SNR), signal-to-background ratio (SBR) and small pixel size [7, 12, 17]. The corresponding uncertainty is estimated using bootstrap replicas of the original data set, as discussed elsewhere [12, 17, 18].

3. SPECTRAL PROPERTIES AND MULTICOLOR IMAGING OF NANOCRYSTAL

Core/shell (CdSe/ZnS) nanocrystals were synthesized as previously described [9, 19] and dissolved in butanol. We used different batches of different diameters, which are supposed to be defined to within 5% as checked by transmission electron microscopy [9, 19].
Mixture of diluted samples (down to 10^{-6} the stock concentration) were deposited on cleaned glass coverslip as previously described [12], resulting in random distribution of NCs. Semiconductor nanocrystals have broad excitation spectra that go far into the UV region, which allows the use of a common excitation wavelength well separated from the emission range. In the following experiments, we used the 488 nm laser line of an Argon ion laser source. In addition, their emission spectra are relatively narrow even at room temperature (on the order of 30-40 nm FWHM) and symmetric, as illustrated on Figure 2.
Individual nanocrystals of a given sample have even narrower emission spectra (15-25 nm), as illustrated by a few examples taken with the full-spectrum mode setup of Fig. 1. In practice, it is possible to separate two partially overlapping nanocrystal spectra by fitting two Lorentzian, if their peak emission wavelengths are distant by more than half their FWHM.

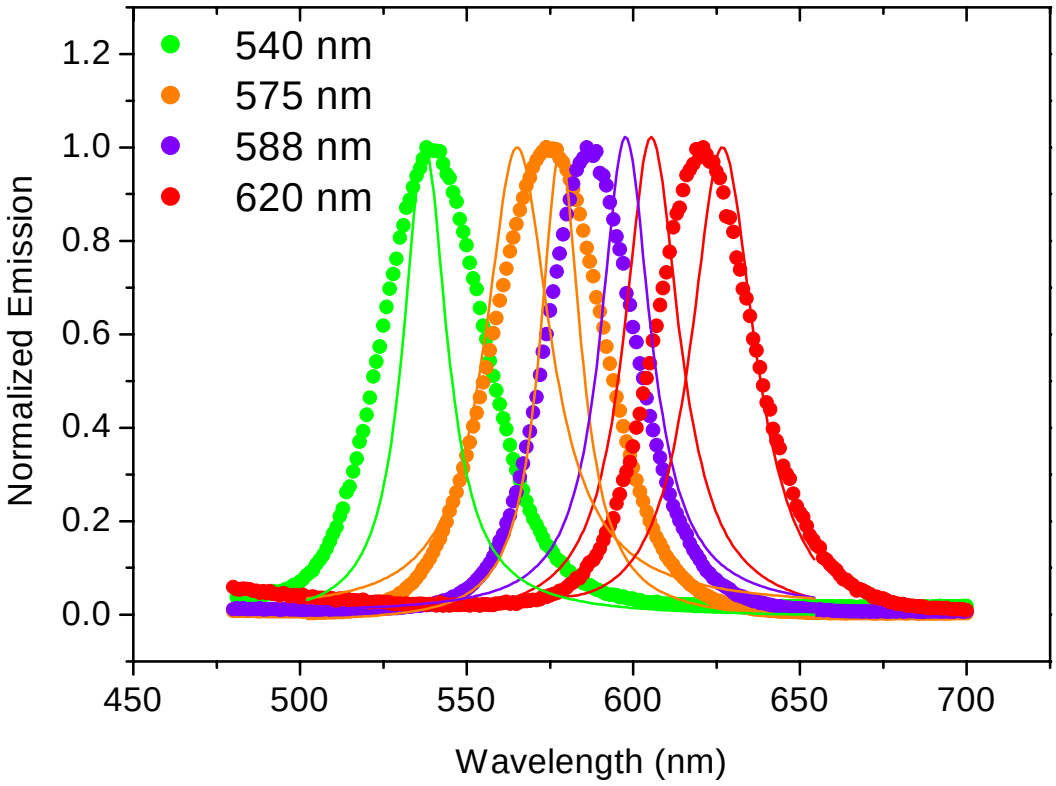

Figure 2: Normalized bulk emission spectra of 4 different NC samples (large dots) obtained with a standard spectrofluorimeter, superimposed with individual nanocrystals spectra (thin curves) as obtained with our multicolor imaging setup using the integrated data of 11x11 pixels and an integration time of 100 ms per pixel (200 nW incident excitation power). FWHM of bulk spectra are of the order of 30 nm: 34, 37, 34 and 32 nm, respectively for the 540, 575, 588 and 620 nm emissions. Peak ± FWHM of individual spectra from left to right (in nm): 537 ± 16, 565 ± 24, 578 ± 15, 598 ± 18, 605 ± 20, 627 ± 24.

However bright and resistant to photobleaching they might be, nanocrystals suffer from a major drawback for confocal (i.e. raster scanning) imaging. Indeed, they exhibit a complex pattern of intermittency [20-23], which results in a patchy image of the excitation PSF, as built up from the fluorescence emitted by a single nanocrystal. Figure 3 gives an example of multicolor imaging of a mixture of 4 batches exhibiting striking example of "blinking" nanocrystals.

Some ambiguity in this image results from the possible close spectra of nearby NCs, which would show up as overlapping PSFs. In order to distinguish this situation (of colocalization) from the mere observation of a single nanocrystal having a spectrum spread over the two selected spectral bands, it is necessary to take advantage of the full-spectrum information, as is illustrated for cases a and b in Fig. 3.

Spectra of two 11x11 pixels covering the two PSFs are shown on Figure 4. It is clear that case a corresponds to a single nanocrystal showing up in the false-color channel red and blue (spectrum: 586 ± 6 nm), whereas case b corresponds to two overlapping nanocrystals (spectra: 546 ± 10 and 602 ± 10 nm).

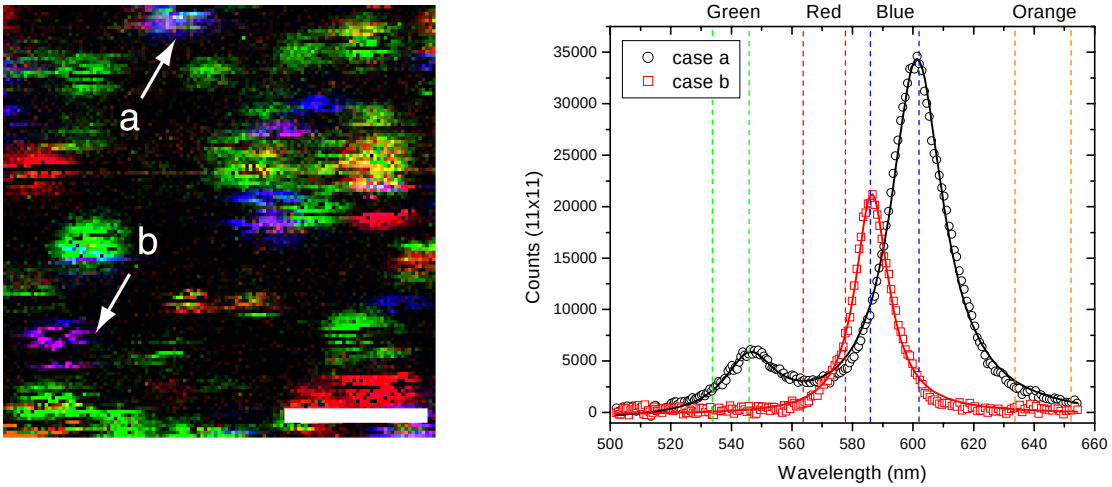

Figure 3: Multicolor imaging of a mixture of 4 NC batches (bulk spectra as indicated in Fig. 2). The area corresponds to a 3 x 3 μm^2 scan (bar indicates 1 µm) using 128 steps. Incident laser power: 200 nW, integration time: 100 ms per pixel. 4 spectral bands were selected as discussed in the text and false-colored (green: 540 ± 6, red: 571 ± 7, blue: 594 ± 8, orange: 643 ± 9). Some overlapping NCs are clearly visible in this contrast-enhanced image (case a, spectrum: 586 ± 6 nm), as well as cases of nanocrystals appearing simultaneously in the blue and red false-color channels (violet, case b, spectra: 546 ± 10 and 602 ± 10 nm).

Figure 4: Spectra of two different 11x11 pixels area of Fig. 3. Recorded spectra are displayed as scatter plots, with the best Lorentzian fits indicated by continuous curves. Boundaries of spectral bands used to build the false-color image planes of Fig. 3 are indicated by dashed vertical lines. Case a correspond to two nearby NCs whose PSFs overlap over most of their physical extension, but with clearly separated spectra (and different emission intensity). Case b corresponds to a single NC whose spectrum overlaps the two chosen bands used to build the red and blue image plane.

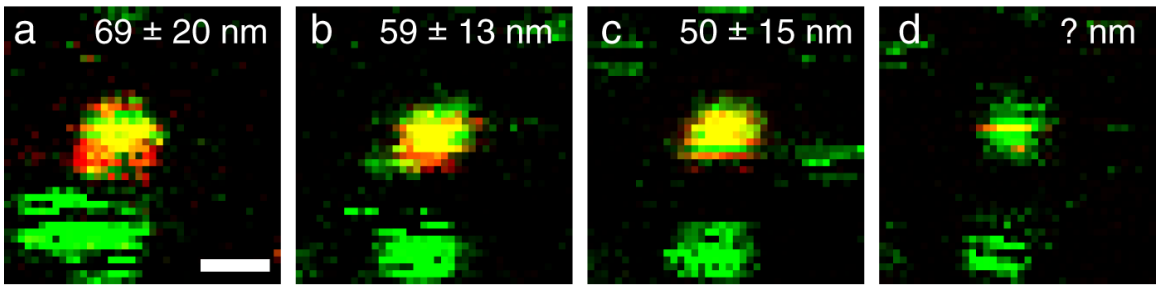

Figure 5: Repeated dual-color imaging of the same 2x2 μm^2 area of a mixture of green and red NCs, excited at 488 nm (incident excitation power: 200 nW, integration time: 50 ms, pixel size: 50 nm). The overall scan duration is about 80 s and the next scan is started almost immediately. Bar indicates 500 nm. The measured distance in each case is indicated with its corresponding 95 % confidence limit error bar as obtained with 1000 bootstrap simulations. Scan d gives a single stripe of signal for the red nanocrystal, so that no position can be determined for this NC. In subsequent scans, this NC gives more complete PSF images.

4. COLOCALIZATION RESULTS

Examples of NC colocalization using the approach exposed in this paper have already been presented elsewhere [12, 17]. Distance measurements down to 25 nm, with a resolution of a few nanometers can be achieved, as long as the scanned NCs do not exhibit too strong intermittency.
Intermittency of the fluorescence emitted by NCs leads to larger uncertainties on the position of the corresponding PSFs compared to non-blinking probes like fluorescent beads that we used in other demonstrations of ultrahigh-resolution colocalization [12, 17]. The reason is not only the reduction of the number of pixels above background available for the PSF fit, but rather more the complete change of probability distribution for each pixel value. This probability distribution is no more a Poisson distribution with mean equal to the value of the local excitation PSF, but a convolution of this and the "on" and "off" time probability distributions. Simulations performed using various probability distributions reported in the literature (exponential [22] or power law [23]), and as observed in our laboratory (data not shown), yielded uncertainties compatible with the values obtained by bootstrap estimation.
To experimentally assess the performance of colocalization studies using nanocrystals, we used the simpler APD (Fig. 1) setup that allows only dual-channel recording. As a consequence, we also limited ourselves to a mixture of green (Emission: 540 nm) and red (Emission: 620 nm) NCs. Since most NCs build up a patchy PSF due to blinking as illustrated in Fig. 3, we decided to estimate the uncertainty on the PSF position measurement by comparing several images of the same area recorded under the same conditions. Figure 5 shows a typical result of this kind of experiment.

The measured distances between the fitted position of each NC varies within the uncertainty computed in each case, which shows that our error bar estimation is robust. However, it also points to the serious problems that can be faced in case of severe blinking, if repeated imaging is not possible.

5. DISCUSSION

Nanocrystals are very attractive fluorescent probes for their ability to be excited by a common wavelength, their narrow spectra and seemingly immunization against photobleaching. Used in wide-field imaging, their intermittency would be of little influence, except to reduce their measured emission yield. In confocal microscopy, however, where the sample (or the beam) is raster scanned, "blinking" results in the diffraction spot corresponding to each individual NC to look patchy. In the worst case, position determination by fitting the PSF with a 2D Gaussian is impossible leading to a complete failure of the ultrahigh-resolution approach presented in this paper.
As rare cases of non-blinking, colocalized NCs, have convinced us, however, ultrahigh-resolution colocalization biological applications of NCs are promising if their photophysical properties can be improved. A possible way for reducing blinking would consist of artificially clustering NCs into aggregates of a few individuals, in order to average their intensity fluctuations. However, possible quenching or other photophysical effects could be introduced [24]. Progress in the synthesis of more efficient NCs is to be expected from the large community now involved in this type of research.
For static observations, the problems arising from severe blinking can be partially compensated for by the ability to scan precisely the same area with nanometer resolution, or use triangulation to fill gaps in a given UHRC measurement. We are currently using this approach to improve the resolution of gene mapping and DNA-binding proteins [25].

7. ACKNOWLEDGMENTS

We thank Tsing-Hua Her, Ted Laurence and Alois Sonnleitner for useful discussions and help with the optics. This work was supported by the National Institutes of Health, National Center for Research Resources, Grant No. 1 R01 RR1489101, through the U.S. Department of Energy under Contract No. DE-AC03-76SF00098.
XM is a Human Frontier Science Program Postdoctoral Fellow.

8. REFERENCES

1. J. G. McNally, T. Karpova, J. Cooper, and J. A. Conchello, "Three-Dimensional Imaging by Deconvolution Microscopy,", *Methods* **19**, pp. 373-385, 1999.
2. E. G. Cragg and P. T. So, "Lateral resolution enhancement with standing evanescent waves," *Optics Letters* **25**, pp. 46-48, 2000.
3. P. Edelman and C. Cremer, "Improvement of confocal Spectral Precision Distance Microscopy (SPDM)," *SPIE Proceedings* **3921**, Optical Diagnostics of Living Cells III, 2000.
4. J. T. Frohn, H. F. Knapp, and A. Stemmer, "True optical resolution beyond the Rayleigh limit achieved by standing wave illumination," *Proceedings of the National Academy of Sciences USA* **97**, pp. 7232-7236, 2000.
5. M. G. L. Gustafsson, D. A. Agard, and J. W. Sedat, "I5M: 3D widefield light microscopy with better than 100 nm axial resolution," *Journal of Microscopy* **195**, pp. 10-16, 1999.
6. T. A. Klar, S. Jakobs, M. Dyba, A. Egner, and S. W. Hell, "Fluorescence microscopy with diffraction resolution barrier broken by stimulated emission," *Proceedings of the National Academy of Sciences USA* **97**, pp. 8206-8210, 2000.
7. N. Bobroff, "Position measurement with a noise-limited instrument," *Review of Scientific Instruments* **57**, pp. 1152-1157, 1986.
8. E. Betzig, "Proposed method for molecular optical imaging," *Optics Letters* **20**, pp. 237-239, 1995.
9. A. P. Alivisatos, "Semiconductor Clusters, Nanocrystals, and Quantum Dots," *Science* **271**, pp. 933-937, 1996.
10. M. J. Bruchez, M. M. Moronne, P. Gin, S. Weiss, and P. A. Alivisatos, "Semiconductor Nanocrystals as Fluorescent Biological Labels," *Science* **281**, pp. 2013-16, 1998.
11. W. C. W. Chan and S. Nie, "Quantum Dot Bioconjugates for Ultrasensitive Nonisotopic Detection," *Science* **281**, pp. 2016-18, 1998.
12. T. D. Lacoste, X. Michalet, F. Pinaud, D. S. Chemla, A. P. Alivisatos, and S. Weiss, "Ultrahigh-resolution multicolor colocalization of single fluorescent probes," *Proceedings of the National Academy of Sciences USA* **97**, pp. 9461–9466, 2000.
13. T. Schmidt, G. J. Schütz, W. Baumgartner, H. J. Gruber, and H. Schindler, "Characterization of Photophysics and Mobility of Single Molecules in a Fluid Lipid Membrane.," *Journal of Physical Chemistry* **99**, pp. 17662-17668, 1995.
14. T. Schmidt, G. J. Schütz, W. Baumgartner, H. J. Gruber, and H. Schindler, "Imaging of single molecule diffusion," *Proceedings of the National Academy of Sciences USA* **93**, pp. 2926-2929, 1996.
15. T. Ha, T. Enderle, D. S. Chemla, and S. Weiss, "Dual-molecule spectroscopy: Molecular rulers for the study of biological macromolecules," *IEEE Journal of Selected Topics in Quantum Electronics* **2**, pp. 1115-1128, 1996.
16. U. Kubitscheck, T. Kues, and R. Peters, "Visualization of Nuclear Pore Complex and Its Distribution by Confocal Laser Scanning Microscopy," in *Confocal Microscopy, Methods in Enzymology* **307**, P. M. Conn, Ed. San Diego: Academic Press, 1999, pp. 207-230.
17. X. Michalet, T. D. Lacoste, and S. Weiss, "Ultrahigh-resolution colocalization of single fluorescent probes," *Methods*, in press.
18. B. Efron and R. J. Tibshirani, *An Introduction to the Bootstrap*, vol. 57: CRC Press, 1994.
19. X. G. Peng, M. C. Schlamp, A. V. Kadavanich, and A. P. Alivisatos, "Epitaxial growth of highly luminescent CdSe/CdS core/shell nanocrystals with photostability and electronic accessibility," *Journal of the American Chemical Society* **119**, pp. 7019-7029, 1997.
20. S. A. Empedocles, D. J. Norris, and M. G. Bawendi, "Photoluminescence Spectroscopy of Single CdSe Nanocrystallite Quantum Dots," *Physical Review Letters* **77**, pp. 3873-3876, 1996.
21. A. L. Efros and M. Rosen, "Random telegraph signal in the photoluminescence intensity of a single quantum dot," *Physical Review Letters* **78**, pp. 1110-13, 1997.
22. U. Banin, M. Bruchez, A. P. Alivisatos, T. Ha, S. Weiss, and D. S. Chemla, "Evidence for a thermal contribution to emission intermittency in single CdSe/CdS core/shell nanocrystals," *Journal of Chemical Physics* **10**, pp. 1-7, 1999.
23. M. Kuno, D. P. Fromm, H. F. Hamann, A. Gallagher, and D. J. Nesbitt, "Nonexponential "blinking" kinetics of single CdSe quantum dots: A universal power law behavior," *Journal of Chemical Physics* **112**, pp. 3117-3120, 2000.

24. C. R. Kagan, C. B. Murray, M. Nirmal, and M. G. Bawendi, “Electronic Energy Transfer in CdSe Quantum Dot Solids,” *Physical Review Letters* **76**, pp. 1517-1520, 1996.
25. X. Michalet, R. Ekong, F. Fougerousse, S. Rousseaux, C. Schurra, N. Hornigold, M. v. Slegtenhorst, J. Wolfe, S. Povey, and A. Bensimon, “Dynamic Molecular Combing: Stretching the Whole Human Genome for High-Resolution Studies,” *Science* **277**, pp. 1518-1523, 1997.